IOPscience iopscience.iop.org

Home Search Collections Journals About Contact us My IOPscience

Thermal transport in isotopically disordered carbon nanotubes: a comparison between Green's functions and Boltzmann approaches

This article has been downloaded from IOPscience. Please scroll down to see the full text article.

2009 J. Phys.: Condens. Matter 21 245302

(http://iopscience.iop.org/0953-8984/21/24/245302)

View the table of contents for this issue, or go to the journal homepage for more

Download details:
IP Address: 129.252.86.83
The article was downloaded on 29/05/2010 at 20:10

Please note that terms and conditions apply.

J. Phys.: Condens. Matter **21** (2009) 245302 (11pp) doi:10.1088/0953-8984/21/24/245302

Thermal transport in isotopically disordered carbon nanotubes: a comparison between Green's functions and Boltzmann approaches

G Stoltz[1], **M Lazzeri**[2] **and F Mauri**[2]

[1] Université Paris Est, CERMICS, Project-team MICMAC, INRIA-Ecole des Ponts, 6 & 8 Avenue Pascal, F-77455 Marne-la-Vallée Cedex 2, France
[2] IMPMC, Universités Paris 6 et 7, CNRS, IGPG, 140 rue de Lourmel, F-75015 Paris, France

E-mail: stoltz@cermics.enpc.fr

Received 14 January 2009, in final form 24 March 2009
Published 21 May 2009
Online at stacks.iop.org/JPhysCM/21/245302

Abstract

We present a study of the phononic thermal conductivity of isotopically disordered carbon nanotubes. In particular, the behaviour of the thermal conductivity as a function of the system length is investigated, using Green's function techniques to compute the transmission across the system. The method is implemented using linear scaling algorithms, which allow us to reach systems of lengths up to $L = 2.5\ \mu$m (with up to 200 000 atoms). As for 1D systems, it is observed that the conductivity diverges with the system size L. We also observe a dramatic decrease of the thermal conductance for systems of experimental sizes (roughly 80% at room temperature for $L = 2.5\ \mu$m), when a large fraction of isotopic disorder is introduced. The results obtained with Green's function techniques are compared to results obtained with a Boltzmann description of thermal transport. There is a good agreement between both approaches for systems of experimental sizes, even in the presence of Anderson localization. This is particularly interesting since the computation of the transmission using Boltzmann's equation is much less computationally expensive, so that larger systems may be studied with this method.

(Some figures in this article are in colour only in the electronic version)

1. Introduction

Carbon nanotubes (CNTs) are very interesting materials for nanoscale electronic devices due to their outstanding mechanical and electrical (depending on their chirality, CNTs can be semiconducting or metallic) properties. Recently, it was also discovered that CNTs have very good thermal properties, as measured experimentally for individual single-walled carbon nanotubes (Yu *et al* 2005) or as estimated by computer simulations. At room temperature, the thermal conductance of carbon nanotubes seems to be dominated by the phononic contribution, even for metallic carbon nanotubes (Hone *et al* 1999, Yamamoto *et al* 2007).

Thermal properties are usually investigated using Fourier's law. For nonequilibrium steady states where the system is put in contact with two reservoirs at different temperatures, there is a net energy flow from the hotter to the colder reservoir. The heat current density $\mathbf{J}$ is proportional to the temperature gradient

$$\mathbf{J} = \kappa \nabla T, \tag{1}$$

κ being the thermal conductivity (a tensor, in general). Denoting by ΔT the temperature difference between the reservoirs, and by L the system size in the direction of the temperature gradient

$$\kappa = \frac{|\mathbf{J}|L}{\Delta T},$$

provided the temperature profile is linear. For usual three-dimensional materials, the thermal conductivity does not depend on the system size, and so it is a well-defined

 © 2009 IOP Publishing Ltd Printed in the UK

thermodynamical quantity. The situation is different for one-dimensional (1D) systems, for which the thermal flux is related to the transmission function of phonons from one reservoir to the other. For defect-free periodic one-dimensional harmonic systems, there is no phonon scattering mechanism. Those systems can sustain a current which does not depend on the system's length (Rieder *et al* 1967), so that $|\mathbf{J}|/\Delta T$ is constant. The thermal conductivity therefore diverges as L, and is not well defined. In general, one-dimensional (1D) systems in which scattering processes can take place should exhibit an intermediate scaling $|\mathbf{J}|/|\Delta T| \sim L^{-\alpha}$ with $0 < \alpha < 1$, in which case the thermal conductivity is again not well defined. For the thermal conductivity to be well defined and Fourier's law to hold, the current should decrease as $|\mathbf{J}|/|\Delta T| \sim L^{-1}$.

The theoretical and numerical results of heat transport in 1D chains are not always acknowledged in computational studies of thermal conductivities of CNTs. There have been many studies on the (non-) validity of Fourier's law in one-dimensional chains. There are two important review papers on this topic, written either from a mathematical (Bonetto *et al* 2000) or a physical (Lepri *et al* 2003) viewpoint.

It is believed that CNTs should have a behaviour reminiscent of 1D systems, although such claims should be backed up by more systematic studies. The dependence of the CNT conductivities on the system length should therefore be a major and primary concern in any study of the thermal conductance. Only very few experimental studies on the length dependence of the thermal conductance of carbon nanotubes are available to our knowledge (see, for instance, (Wang *et al* 2007) and (Chang *et al* 2008)), and numerical results are still rare. More importantly, Fourier's law, which is not valid in general for 1D systems, is sometimes assumed to hold to interpret experimental measurements in order to extract conductivities (Pop *et al* 2006).

In order to have a well-defined conductivity, a necessary condition (which may not be sufficient) is that some scattering mechanisms can take place, so that the thermal flux is reduced. Several scattering mechanisms exist in actual materials, which may be intrinsic, as for inelastic anharmonic phonon–phonon scattering, or extrinsic, as for elastic phonon scattering with defects. Experimental results showed that CNTs of lengths 2.76 μm may exhibit nearly ballistic transport (Yu *et al* 2005). This justifies that anharmonic scattering may be neglected if the elastic scattering processes with defects are important. The most simple defect that can be experimentally controlled is isotope disorder, which amounts here to replacing the usual ^{12}C atom by one of its ^{13}C isotope. CNTs with isotope disorder have already been synthesized (Simon *et al* 2005) and experimental results on boron nitride tubes (Chang *et al* 2006) showed that isotope disorder could lead to dramatic changes in the thermal conductivity. Moreover, isotopically disordered harmonic systems are also the simplest systems that can be treated exactly with quantum statistics. However, it may already be expected that isotope defects will not be able to remove the divergent thermal conductivity, as already mentioned in Mingo and Broido (2005b).

There are several methods to compute the thermal conductance of isotopically disordered harmonic systems using quantum statistics (we therefore disregard molecular dynamics techniques which give only results within the classical framework). These systems exhibit Anderson localization (Matsuda and Ishii 1970), which arises from an interference effect of different scattering paths, and is thus a manifestation of the undulatory nature of the phonon vibrations. The Green's function technique is then a very appealing method to compute the thermal conductance in those systems, since it gives the exact transmission, has a computational cost scaling linearly with the system length and is straightforward to parallelize since transport is coherent. This allows us to reach systems of lengths up to $L = 2.5$ μm (with up to 200 000 atoms). A Boltzmann approach, which describes the evolution of the phonon distribution and therefore treats phonons as particles and not as waves, gives only an average description of the phonon flows in the system. It cannot account for the Anderson localization of states, and it is therefore unclear whether it can provide a good approximation to the exact transmission. A Boltzmann treatment of the transmission is, however, very interesting since the method is computationally less expensive (no averages over the disorder realizations have to be taken, the computational scaling with respect to the CNT index is more favourable and the inclusion of anharmonic scattering processes is easier than for Green's functions).

In this paper, we will address three problems, systematically studying the length dependence of the thermal conductivity with Green's function techniques:

(i) does a well-defined conductivity (independent of the length) exist for harmonic disordered CNTs, or is the thermal transport anomalous? The theoretical results on heat transport in 1D chains suggest that the transport is anomalous, but can the asymptotic divergence $\kappa(L) \sim L^{\beta}$ be estimated, or should incredibly long tubes be considered before such a regime is found?
(ii) how much is the thermal conductance reduced by isotopic disorder? How does this decrease depend on the temperature?
(iii) in order to reach even larger systems (larger diameters and/or lengths), a third question is whether the Boltzmann approach to thermal transport is a good approximation for CNTs *of experimental lengths*?

This paper is organized as follows. We present briefly the notation and the numerical method in section 2. We then turn to isotopically disordered one-dimensional chains in section 3, in order to test the validity of the Boltzmann approach in this simple case. Section 4 presents our new results on the systematic study of the length dependence of the thermal conductivity for CNTs. A conclusion is presented in section 5.

2. Models for thermal transport

We recall in this section two important models of transport: (i) the Green's function approach, which solves the model in its full atomistic details, and is exact for harmonic systems and (ii) the computationally less expensive but more approximate Boltzmann treatment. Both approaches will be used here to compute the decrease of the thermal conductance arising

from a disordered region embedded in an otherwise perfect medium. We remark that the Green's function treatment gives the exact transmission for a *given realization of the mass disorder*. Therefore, averages over the disorder realizations have to be performed, unless the transmission function does not vary much from one disorder realization to another. In contrast, the Boltzmann approach already gives some average transmission.

2.1. The Green's function treatment of thermal transport

2.1.1. Description of layered one-dimensional systems. Coherent thermal transport, presented in a pedagogical fashion in Zhang *et al* (2007), involves expressions very similar to the usual expressions for electronic transport (Datta 2005, 2000). The lattice thermal conductance arises from phonons (Ashcroft and Mermin 1976, Baroni *et al* 2001), which are quantized displacements of harmonic lattices. We consider an infinitely extended system as depicted in figure 1. The Hamiltonian is

$$H(\mathbf{q},\mathbf{p}) = \tfrac{1}{2}\mathbf{q}^{\mathrm{t}} K \mathbf{q} + \tfrac{1}{2}\mathbf{p}^{\mathrm{t}} M^{-1}\mathbf{p},$$

where the infinite-dimensional vectors $\mathbf{q} = (\ldots, \mathbf{q}_{i,1}, \ldots, \mathbf{q}_{i,N}, \mathbf{q}_{i+1,1}, \ldots)^{\mathrm{t}}$, $\mathbf{p} = (\ldots, \mathbf{p}_{i,1}, \ldots, \mathbf{p}_{i,N}, \mathbf{p}_{i+1,1}, \ldots)^{\mathrm{t}}$ stand, respectively, for displacements and momenta. The first index refers to the cell to which the atom belongs and the second indexes the atom within a cell. The cell in question can be the periodic unit cell used to generate the system, but it may also be some convenient supercell (see below). The infinite-dimensional matrix M is the (diagonal) mass matrix of the system. The matrix K is the interatomic force constant matrix. It is assumed to be short ranged in the following, so that an atom interacts only with atoms located in a few neighbouring unit cells. Changing coordinates to mass weighted coordinates, the transport properties of the system can in fact be completely characterized by the harmonic matrix

$$A = M^{-1/2} K M^{-1/2}. \tag{2}$$

We restrict ourselves in this study to a disordered region embedded in a perfect medium (see figure 1). The case of mass disorder is then dealt with by considering the mass of the particles to be randomly distributed. In the most physical case, namely isotopic disorder, the probability to have the mass m at a given site is $1-c$ and the probability to have a mass $m+\Delta m$ is c, where $0 \leqslant c \leqslant 1$ denotes the disorder concentration. The assumptions on the system imply that the mass matrix is of the general form

$$M = \begin{pmatrix} M_{\mathrm{L}} & 0 & 0 \\ 0 & M_{\mathrm{sys}} & 0 \\ 0 & 0 & M_{\mathrm{R}} \end{pmatrix}, \tag{3}$$

where in M_{L} and M_{R} all the masses are equal to m, while in M_{sys} they are randomly distributed.

Carbon nanotubes are quasi-one-dimensional systems, that is, systems of finite size in the transverse directions and (infinitely) extended in the remaining direction. We consider a fundamental supercell (a layer) composed of possibly several unit cells. The number of cells in this fundamental structure is determined by the condition that an atom in a layer interacts only with atoms in the two adjacent layers. The harmonic matrix therefore has the generic block tridiagonal shape

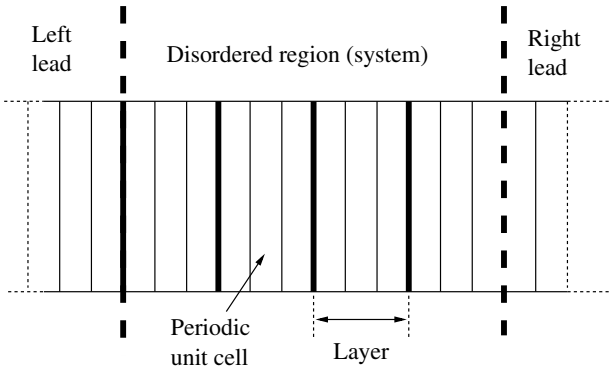

Figure 1. View of a layered 1D system. The infinite system is decomposed into three regions: a semi-infinite left lead, a semi-infinite right lead (which are both assumed to be perfect) and a finite central disordered region. Assuming here that the atoms in the periodic unit cell interact with atoms located in the three neighbouring cells on each side, a fundamental 'supercell', called a layer, can be considered. Atoms in such a layer interact only with atoms in the two adjacent layers.

$$A = \begin{pmatrix} A_{\mathrm{L}} & \mathfrak{T}_{\mathrm{L}} & 0 \\ \mathfrak{T}_{\mathrm{L}}^{\mathrm{t}} & A_{\mathrm{sys}} & \mathfrak{T}_{\mathrm{R}} \\ 0 & \mathfrak{T}_{\mathrm{R}}^{\mathrm{t}} & A_{\mathrm{R}} \end{pmatrix}. \tag{4}$$

The (infinite) subsystems associated with the semi-infinite matrices A_{L} and A_{R} represent some reservoirs to which the (finite) system A_{sys} is coupled through the interaction terms $\mathfrak{T}_{\mathrm{L}}, \mathfrak{T}_{\mathrm{R}}$ (for a matrix $\mathcal{M}$, $\mathcal{M}^{\mathrm{t}}$ denotes the transpose matrix, while $\mathcal{M}^{\dagger}$ denotes the Hermitian conjugate of $\mathcal{M}$ in the following). If N_{layers} is the number of layers composing the disordered region, there are $N_{\mathrm{at}} N_{\mathrm{layers}}$ atoms in the central part, and the matrix A_{sys} is of size $3N_{\mathrm{at}} N_{\mathrm{layers}} \times 3N_{\mathrm{at}} N_{\mathrm{layers}}$.

2.1.2. Heat current in terms of Green's functions. The Green's function of the whole system is defined as

$$G^{+}(\omega) = \lim_{\eta \to 0} (\omega^2 + \mathrm{i}\eta - A)^{-1}$$

when this limit exists (Jaksic 2006). In numerical computations, the parameter η is a small positive number. The effective Green's function for the central region is

$$G^{+}_{\mathrm{sys}}(\omega) = \lim_{\eta \to 0} \left(\omega^2 + \mathrm{i}\eta - A_{\mathrm{sys}} - \Sigma^{+}_{\mathrm{L}}(\omega) - \Sigma^{+}_{\mathrm{R}}(\omega)\right)^{-1}, \tag{5}$$

where the self-energies

$$\Sigma^{+}_{\alpha}(\omega) = \lim_{\eta \to 0} \mathfrak{T}^{\mathrm{t}}_{\alpha} (\omega^2 + \mathrm{i}\eta - A_{\alpha})^{-1} \mathfrak{T}_{\alpha} \qquad (\alpha = \mathrm{L}, \mathrm{R})$$

model the coupling of the system with the contacts. In particular, the imaginary part of the self-energy is usually associated with some lifetime (due to phonons flowing out of the central region). This is maybe more easily understood in the quantum Langevin framework, where the self-energy is the Fourier transform of the friction kernel (Dhar and Roy 2006).

When there are no incoherent scattering processes, the current is given as the superposition of phonons going from the left reservoir to the right one, minus the flow of phonons going from the right reservoir to the left one. When the reservoirs are at different temperatures (respectively, $T_{\rm L}$ and $T_{\rm R}$), the heat current flowing through the system is (Datta 2005, Zhang *et al* 2007, Dhar and Roy 2006)

$$J(T_{\rm L}, T_{\rm R}) = \int_0^{+\infty} \frac{\hbar\omega}{2\pi} \mathcal{T}(\omega)(f_{T_{\rm L}}(\omega) - f_{T_{\rm R}}(\omega))\,{\rm d}\omega, \qquad (6)$$

where the transmission factor $\mathcal{T}(\omega)$ is

$$\mathcal{T}(\omega) = {\rm Tr}[\Gamma_{\rm L}^{+}(\omega) G_{\rm sys}^{+}(\omega) \Gamma_{\rm R}^{+}(\omega) (G_{\rm sys}^{+}(\omega))^{\dagger}]. \qquad (7)$$

In the above expressions, $\Gamma_{\alpha}^{+}(\omega) = -2{\rm Im}(\Sigma_{\alpha}^{+}(\omega))(\alpha = {\rm L}, {\rm R})$ is related to the imaginary part of the self-energies and the functions $f_{\rm T}$ are the Bose–Einstein distributions

$$f_{\rm T}(\omega) = \left(\exp\left(\frac{\hbar\omega}{k_{\rm B}T} \right) - 1 \right)^{-1}.$$

The expression of the thermal conductance is exact since the system is harmonic. The practical computation of the transmission is presented, for instance, in appendix A of Stoltz *et al* (2008).

Introducing $t(\omega) = \Gamma_{\rm L}(\omega)^{1/2} G_{\rm sys}^{+}(\omega) \Gamma_{\rm R}(\omega)^{1/2}$, the transmission can be rewritten as $\mathcal{T}(\omega) = {\rm Tr}(t(\omega)t(\omega)^{\dagger})$. It is therefore nonnegative. In fact, when there is no disorder, the transmission is ballistic and equal to the number of conducting channels at this pulsation. In the presence of mass disorder, the transmission is lower than the ballistic transmission.

2.1.3. Thermal conductance and thermal conductivity. The thermal conductance associated with the heat current (6) is obtained in the limit $\Delta T = T_{\rm R} - T_{\rm L} \to 0$ as

$$g(T) = \lim_{\Delta T \to 0} \frac{J\left(T + \frac{\Delta T}{2}, T - \frac{\Delta T}{2}\right)}{\Delta T} = \int_0^{+\infty} \frac{\hbar\omega}{2\pi} \mathcal{T}(\omega) \frac{\partial f_T(\omega)}{\partial T}\,{\rm d}\omega. \qquad (8)$$

A remarkable fact about the heat current is that the associated thermal conductance is quantized (Rego and Kirczenow 1998), the quanta of thermal conductance being

$$g_0(T) = \frac{\pi^2 k_{\rm B}^2 T}{3h}. \qquad (9)$$

This expression is obtained in the limit $T \to 0$ for a single acoustic branch in the ballistic regime. The quantum of thermal conductance has been experimentally measured (Schwab *et al* 2000). In the following, conductances will most often be normalized with respect to the quantum of thermal conductance:

$$\bar{g}(T) = \frac{g(T)}{g_0(T)}. \qquad (10)$$

The dimensionless quantity $\bar{g}(T)$ is called 'normalized conductance' in the results presented below.

For 1D systems, the thermal conductivity κ is the thermal conductance divided by the system cross section $\mathcal{A}$ and multiplied by the system length L:

$$\kappa = \frac{gL}{\mathcal{A}}. \qquad (11)$$

The notion of cross section depends on the system considered and on the conventions used (see section 4.1 for our conventions in the case of CNTs). From this definition, it is, however, clear that the existence of a well-defined (length-independent) non-vanishing thermal conductivity requires a decrease of the thermal current (or thermal conductance) as $1/L$. Since the thermal conductivity is not well defined *a priori*, the thermal conductance is a much better notion to handle.

The practical computation of the thermal conductance using (8) therefore boils down to computing the transmission factor $\mathcal{T}(\omega)$ given by (7) for the whole phonon spectrum (see appendix A of Stoltz *et al* (2008)).

2.2. The Boltzmann approximation of coherent transport

The Boltzmann method is a less expensive but more approximate method than the Green's function treatment for the computation of the thermal conductance. It allows us to compute conductivities for very long systems, and therefore to study the length dependence of the conductivity. Recent derivations of the Boltzmann equation from microscopic dynamics have been presented in Spohn (2006), Lukkarinen and Spohn (2007) in the so-called kinetic limit (vanishingly small mass disorder or anharmonicities, long time limit, interatomic spacing going to zero). The Boltzmann equation therefore describes some average behaviour of the phonons.

The central object describing this average behaviour is the phonon distribution $n_j(\omega, x, t)$. The index j labels the phonon branch, ω is the phonon pulsation, while x is the position along the system. The quantity $n_j(\omega, x, t)$ therefore counts the number of phonons of pulsation ω in the jth branch at a point x at time t. The evolution of the phonon distribution is governed by the Boltzmann equation, which consists of two terms: (i) a transport term, which models the free flow of phonons through the harmonic system of reference, and (ii) a collision term, which models the rate at which phonons from one branch are scattered into another branch due to the defects and/or impurities in the actual system. Since we do not consider anharmonic effects in this study but only mass defects, the energy is conserved in the collision processes and the only scattering mechanism is the scattering from a phonon in a given branch to a phonon in another branch *at the same energy*.

2.2.1. The Boltzmann equation. For the system introduced in section 2.1.1, a phonon at a wavevector k is an eigenvector of the dynamical matrix of the perfect system. For a given pulsation $\bar{\omega} \geqslant 0$, the associated phononic branches j at this pulsation are all solutions of the equation

$$\omega_j^2(k) = \omega_j^2(-k) = \bar{\omega}^2, \qquad 0 \leqslant j \leqslant 3N_{\rm at}, \qquad (12)$$

for some k in the Brillouin zone. We denote by $N \equiv N(\bar{\omega})$ the number of branches at this pulsation and by $n_{j,\sigma}(\omega, x, t)$ the density of phonons of the jth branch ($j = 1, \ldots, N(\bar{\omega})$ upon reordering). The index $\sigma = \pm 1$ labels the solutions $\omega_j^2(k) = \bar{\omega}^2$ depending on the sign of the phononic velocity: $\sigma = +1$ corresponds to k points such that

$$\omega_j(k_{j,+1}) = \bar{\omega}, \qquad v_j = \frac{\partial \omega_j}{\partial k}(k_{j,+1}) > 0,$$

whereas the velocity is negative at points $k_{j,-1} = -k_{j,+1}$, and is actually equal to $-v_j$.

The Boltzmann equation is

$$\begin{aligned}\left(\partial_t + \sigma\, v_j \partial_x\right) n_{j,\sigma}(\omega, x, t) \\ = \sum_{(j',\sigma') \neq (j,\sigma)} \frac{W_{(j,\sigma),(j',\sigma')}}{v_j} n_{j',\sigma'}(\omega, x, t) \\ - \frac{W_{(j',\sigma'),(j,\sigma)}}{v_{j'}} n_{j,\sigma}(\omega, x, t). \end{aligned} \tag{13}$$

The left-hand side of the above equation is the transport part of the Boltzmann equation. Notice also that ω does not enter explicitly in the above equation. It can therefore be considered as a continuous parameter indexing a set of independent equations.

The matrix $W = [W_{(j,\sigma),(j',\sigma')}]_{1 \leqslant j,j' \leqslant N, \sigma,\sigma' = \pm 1}$ describes the interactions between the branches, i.e. the collision term. It is such that for all $(j, \sigma) \neq (j', \sigma')$:

$$W_{(j,\sigma),(j',\sigma')} \geqslant 0, \qquad W_{(j,\sigma),(j',\sigma')} = W_{(j',\sigma'),(j,\sigma)},$$

$$W_{(j,-\sigma),(j',-\sigma')} = W_{(j',\sigma'),(j,\sigma)}.$$

The above conditions have physical interpretations: (i) the first condition (non-negativity of the matrix elements) means that the scattering term models the decay of phonons of one branch into phonons of another branch; (ii) the second condition ensures the conservation of the total phonon number and (iii) the last condition is some symmetry condition with respect to the propagation direction of phonons. The precise form of the scattering matrix depends on the problem at hand; see below the expression (14) in the case of isotopically disordered lattices.

2.2.2. The collision term. The expression of the scattering matrix are derived from a perturbative approach based on the Fermi golden rule (Tamura 1983, Widulle *et al* 2002, Vandecasteele *et al* 2009):

$$W_{(j,\sigma),(j',\sigma')} = l_0 \frac{\mathrm{Var}(m)}{\langle m \rangle^2} \bar{\omega}^2 \sum_{l=1}^{N_{\mathrm{at}}} |\mathbf{u}^\star_{j,\sigma}(l) \cdot \mathbf{u}_{j',\sigma'}(l)|^2, \tag{14}$$

where $\langle m \rangle$ and $\mathrm{Var}(m) = \langle m^2 \rangle - \langle m \rangle^2$ are the average mass and the variance of the mass disorder, respectively, and l_0 is the length of the unit cell. The three-dimensional vector $\mathbf{u}_{j,\sigma}(l)$ is the part of u_j corresponding to the three degrees of freedom of the lth atom in the unit cell for phonon displacements u_j computed for a perfect lattice.

The scattering term (14) agrees with the mathematical results obtained by the kinetic limit of the microscopic dynamics in the case of a simple one-dimensional chain (Lukkarinen and Spohn 2007). From a numerical viewpoint, the expression (14) is very interesting since it allows an analytic computation of the scattering rates once the phonon spectrum has been computed. Appendix B of Stoltz *et al* (2008) presents the details of the numerical solution of (13) using the scattering term (14).

2.2.3. Transmission properties using the Boltzmann equation. Thermal properties are computed for nonequilibrium steady states where a heat current flows through the system. This is done by setting appropriate boundary conditions and waiting for the system to equilibrate. The boundary conditions for (13) suited to the transmission of a single phonon from the left (hot) reservoir to the right (cold) one, are:

$$n_{j,+}(\omega, 0, t) = 1, \qquad n_{j,-}(\omega, L, t) = 0.$$

The numbers $n_{j,+}(\omega, L, t)$ and $n_{j,-}(\omega, 0, t)$ are, respectively, the proportion of transmitted and reflected phonons. These proportions are computed using the Boltzmann equation and this defines the transmission factor.

When a stationary regime is reached ($\partial_t n_{j,\sigma} = 0$ for all j, σ), the phonon distributions do not depend on time anymore and we drop the variable t in our notations. It is easily seen that the transmission coefficient is independent of the position x, so that

$$T(\omega, x) = N(\omega) \frac{\sum_{j=1}^{N(\omega)} n_{j,+}(\omega, L)\, v_j(\omega)}{\sum_{j=1}^{N(\omega)} v_j(\omega)}.$$

This coefficient is the Boltzmann equivalent of the transmission function $\mathcal{T}(\omega)$ computed using Green's function techniques.

3. Results for one-dimensional chains

Perfect one-dimensional harmonic lattices with nearest-neighbour interactions are described by the Hamiltonian

$$H = \sum_j \frac{p_j^2}{2m} + \frac{1}{2} k (q_{j+1} - q_j)^2.$$

This model fits in the general framework presented in section 2 when taking $N_{\mathrm{at}} = 1$ atoms per unit cell and layers of $N_{\mathrm{layers}} = 1$ unit cell. In this section, we will work in reduced units of mass and length, and consider a one-dimensional chain with unit lattice spacing and particles of mass 1. The ballistic transmission of this model is

$$T(\omega) = \begin{cases} 1 & \text{if } 0 \leqslant \omega \leqslant \omega_{\max}, \\ 0 & \text{otherwise.} \end{cases}$$

Isotopic disorder is modelled by replacing with probability $0 < c < 1$ the mass of a particle by $m(1+\delta)$ with $\delta = \Delta m / m$.

3.1. Heat transport in isotopically disordered harmonic lattices

Heat transport in isotopically disordered harmonic lattices has been thoroughly studied (Matsuda and Ishii 1970, Rubin

and Greer 1971, Casher and Lebowitz 1971, Ishii 1973, O'Connor and Lebowitz 1974). In particular, the case of a finite disordered chain connected to two semi-infinite perfect chains has been considered (Rubin and Greer 1971) and the corresponding theoretical results were rederived from a different perspective and extended in O'Connor and Lebowitz (1974), Dhar (2001). It is suggested in Rubin and Greer (1971) that the thermal conductivity diverges as $\sqrt{L}$ (L being the chain length). This has been shown rigorously (Keller *et al* 1978) for an analogous continuum wave model (open boundary conditions and disorder).

Heuristic arguments can be employed to back up the $\sqrt{L}$ divergence of the thermal conductivity by studying the properties of the transmission function. Denoting explicitly the length dependence of the transmission function by $\mathcal{T}_{\rm L}(\omega)$, the exact transmission decreases exponentially as

$$\mathcal{T}_{\rm L}(\omega) \simeq \exp(-L/l_{\rm loc}(\omega)). \tag{15}$$

The length $l_{\rm loc}$ is the localization length. This result was proved in Matsuda and Ishii (1970) (but earlier obtained in the limit of low concentration of defects (Rubin 1968)). The proof is based on a theorem by Furstenberg on the product of random matrices (Furstenberg 1963). The behaviour of $l_{\rm loc}$ around $\omega^2 = 0$ can also be precised (Matsuda and Ishii 1970, O'Connor and Lebowitz 1974). For isotopic disorder, it can be shown that

$$\lim_{\omega^2\to 0} \frac{1}{\omega^2\, l_{\rm loc}(\omega)} = \frac{{\rm Var}(m)}{\langle m\rangle^2} = \frac{c(1-c)}{4}\frac{\delta^2}{(1+c\delta/2)^2}. \tag{16}$$

This shows that a high frequency implies a shorter localization length and therefore the associated eigenmodes are strongly localized, so that only the low frequency modes contribute to transport; in fact, only a fraction $\mathrm{O}(L^{-1/2})$ of them since

$$\mathcal{T}_{\rm L}(\omega) \simeq \exp\left(-\frac{{\rm Var}(m)}{\langle m\rangle^2} L\omega^2\right)$$

when $\omega \to 0$. This explains therefore the $L^{-1/2}$ decay of the thermal conductance, in view of (8).

3.2. Comparison of the Green's function and Boltzmann treatments

The transmission is computed using the Green's function approach at $N_\omega = 5000$ points uniformly spaced in the range $[0, \omega_{\rm max}]$, with $\eta/\omega_{\rm max}^2 = 10^{-12}$ (the self-energies having an analytical expression, see, for instance, (Economou 2006)). The averages are taken over $N_{\rm disorder} = 100$ realizations of the isotopic disorder for chains of length $L = 10^6$, while $N_{\rm disorder} = 1000$ for $L = 10^5$ and $N_{\rm disorder} = 10^4$ for $L = 10^2$–10^4. The average transmission functions computed from (7) are presented in figure 2 in the case $\delta = 1/12$ and $c = 0.5$. The mass variation δ is the mass variation corresponding to substituting ^{12}C with ^{13}C.

The transmission predicted by the Boltzmann approach can be computed analytically in this simple case since there is only a single branch and there are therefore only two

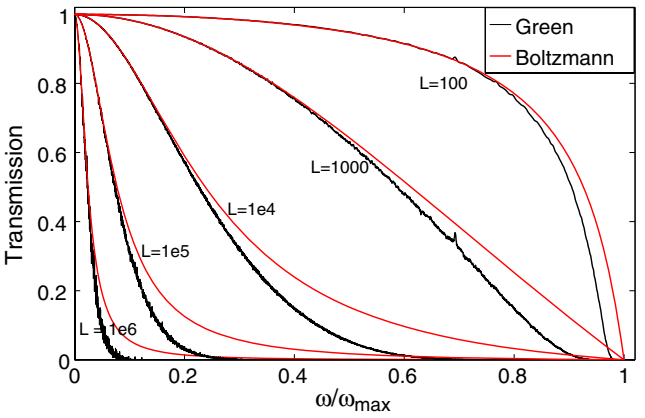

Figure 2. Averaged transmission function $\mathcal{T}_{\rm L}(\omega)$ as a function of ω for different system sizes. From top to down: increasing system sizes from $L = 100$ to 10^6. The (thick) black curves are the transmissions computed with a Green's function approach and the (thin) red curves are obtained from the Boltzmann formula (17).

conducting states for a given pulsation (due to the symmetry $\omega(k) = \omega(-k)$). The transmission is of diffusive type, with

$$T_{\rm L}(\omega) = \left(1 + \frac{L}{l_{\rm Boltz}(\omega)}\right)^{-1}, \tag{17}$$

with

$$\frac{1}{\omega^2\, l_{\rm Boltz}(\omega)} = \frac{{\rm Var}(m)}{\langle m\rangle^2}\left(1 - \frac{\omega^2}{4}\right)^{-1}.$$

Notice that this expression of the transmission agrees at second order in ω with (15) in the limit $\omega \to 0$.

The comparison between the transmissions computed with the Green's function and the Boltzmann approaches shows that the Boltzmann treatment is a reasonable approximation for low frequency modes, but predicts a transmission which is too large for higher frequencies. The critical frequency at which the Boltzmann transmission starts to depart significantly from the Green's function transmission decreases with the system size. Therefore, we expect the conductances to agree in the low temperature regime for all system lengths and the relative error to increase with the system length at larger temperatures where the higher frequency part of the transmission is taken into account.

This is indeed confirmed by the scalings of the normalized thermal conductance (computed using (10)) in figure 3 for different values of $x = \hbar\omega/k_{\rm B}T$. As expected, the asymptotic scaling $L^{-1/2}$ for the thermal conductance is reached for systems long enough when the transmission is computed using the Green's function approach. This could be anticipated since the Green's function results are exact for harmonic systems. Besides, it is observed that the asymptotic regime where the conductance scales as $\bar{g} \sim L^{-1/2}$ is attained for shorter tubes when the temperature is increased. Some of our simulations (not presented here) also showed that longer tube lengths are required for this regime to be attained when the disorder concentration is lower.

On the other hand, the conductances predicted by the Boltzmann approach for systems long enough, are larger than

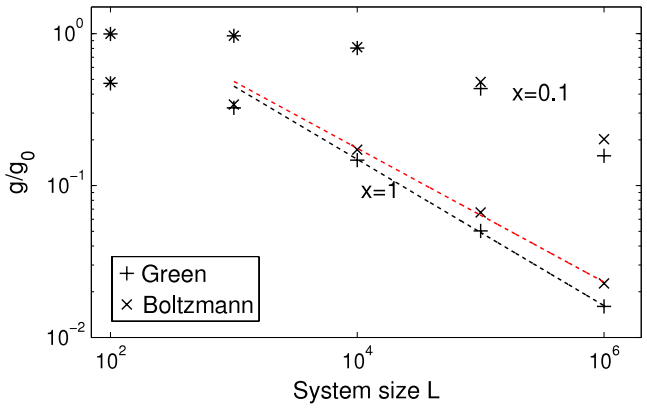

Figure 3. Conductances computed using the Green's function approach and a Boltzmann treatment for two values of $x = \hbar\omega/k_B T$. The asymptotic regime where $\bar{g} \sim L^{-\alpha}$ (dashed lines) is attained only for $x = 1$, with $\alpha \simeq 0.48$ for the Green's function approach and $\alpha \simeq 0.44$ in the Boltzmann case.

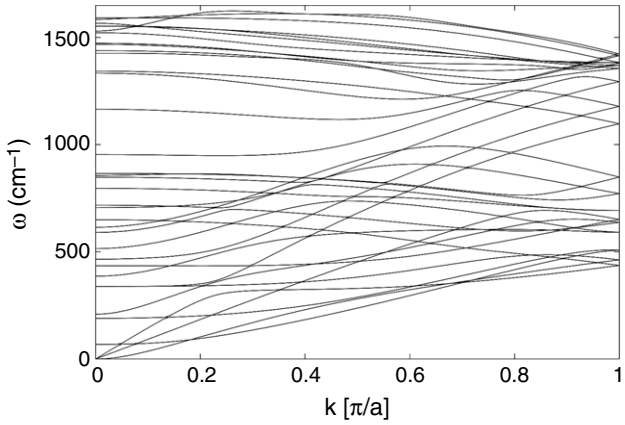

Figure 4. Phonon spectrum of a (5, 5) CNT with *ab initio* computed interatomic forces.

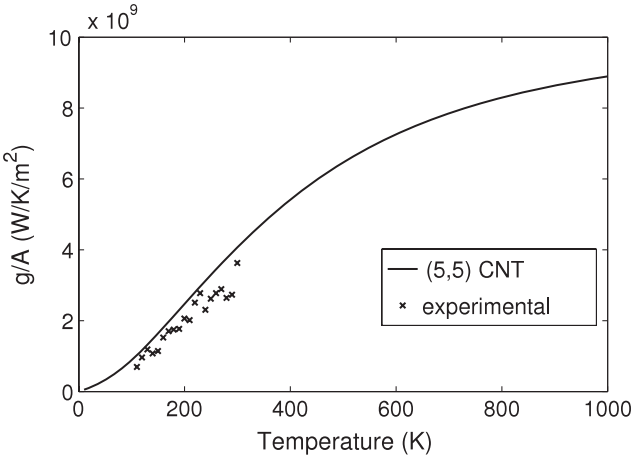

Figure 5. Ballistic conductivity per unit length (expressed in Å), with the cross-sectional area (18). Experimental points taken from Yu *et al* (2005) are also reported.

the conductances obtained with the Green's function approach. The Boltzmann treatment does not predict the right asymptotic scaling either, though the discrepancy is not too large. This is due to the fact that the Boltzmann transmission does not decay fast enough with the system size for larger values of ω.

4. Numerical results for carbon nanotubes

4.1. Description of the model

In the model we use, the tube is simulated using the interatomic force constants (IFCs) computed from density functional theory calculations (Baroni *et al* 2001), using the PWCSF package of the QUANTUM-ESPRESSO distribution (Baroni 000) on a (5, 5) CNT[3]. We restrict ourselves to armchair nanotubes for simplicity. Armchair nanotubes are very important for applications since they are metallic (here we compute only the phononic thermal conductance). We expect the results presented below to be robust with respect to the system chirality, because the ballistic conductance does not change much with the chirality (Mingo and Broido 2005a).

In order to have a block tridiagonal form for the interaction matrix within the *ab initio* model, only interactions within a cutoff radius $R_{\text{cut}} = 15$ Bohr are taken into account. The projection procedure of (Mounet 2005) was used to ensure that acoustic sum rules are satisfied for the truncated IFC matrix. The resulting phonon spectrum is presented in figure 4. As expected, there are four acoustic modes since the flexural mode (starting with a k^2 dispersion law) is doubly degenerate.

We first compare the computed thermal conductance of perfect CNTs and experimental measurements. Actually, a more intrinsic property to compare is the ballistic thermal conductance divided by the cross-sectional surface of the material $g/\mathcal{A}$ (this is the so-called ballistic conductivity per unit length, compare with (11)). The cross-sectional area $\mathcal{A}$ is obtained from a 'fattened' carbon ring:

$$\mathcal{A} = 2\pi Rd = 3nd, \tag{18}$$

where n is the index of the nanotube, R is the radius of the carbon ring and $d = 3.35$ Å (the graphite interlayer separation) is some characteristic length defining the width of the annular domain enclosing the carbon ring. Figure 5 presents a plot of $g/\mathcal{A}$ as a function of the temperature for two CNTs of different indices, as well as a reference curve computed from *ab initio* results and experimental results (Yu *et al* 2005).

The agreement with the experimental results from Yu *et al* (2005) for temperatures around room temperature and below suggests that the present models contain the essential ingredients for describing thermal transport. In particular, other effects (at present not taken into account) such as anharmonic interactions may be neglected in this temperature regime (and for lower temperatures). The measurements from Yu *et al* (2005) have been transformed into conductivities per

[3] The computations were performed using the local density approximation (Ceperley and Alder 1980), norm-conserving pseudo-potentials (Troullier and Martins 1991, Fuchs and Scheffler 1999) and a plane-wave expansion up to 55 Ryd cutoff. Brillouin-zone sampling was performed on a $1 \times 1 \times 32$ Monkhorst–Pack mesh, with a Fermi–Dirac smearing of 0.02 Ryd. The dynamical matrices are calculated on a $1 \times 1 \times 12$ grid of q-points and Fourier interpolation is used to get the dynamical matrices on a finer mesh of q-points. The theoretical radius of the (5, 5) CNT is 6.412 Bohr.

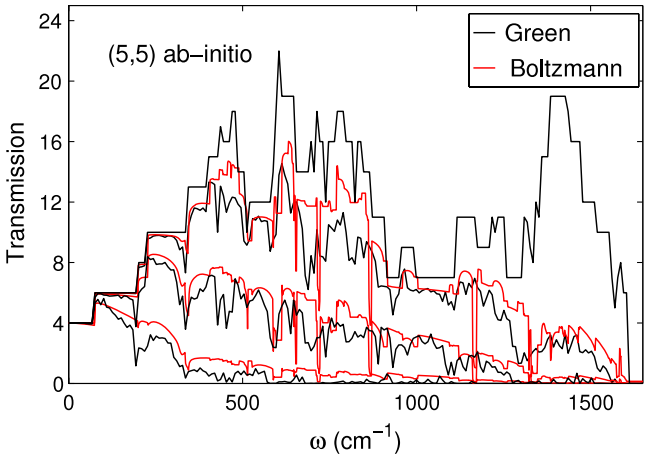

Figure 6. Transmissions obtained with the Green's function formalism (black curves) and the Boltzmann approach (red curves). The line corresponding to the largest transmission is the reference ballistic transmission. The other lines correspond to tubes of different lengths, namely $L = 25$ nm, 249 nm and 2.49 μm, the highest transmissions corresponding to the shortest tubes.

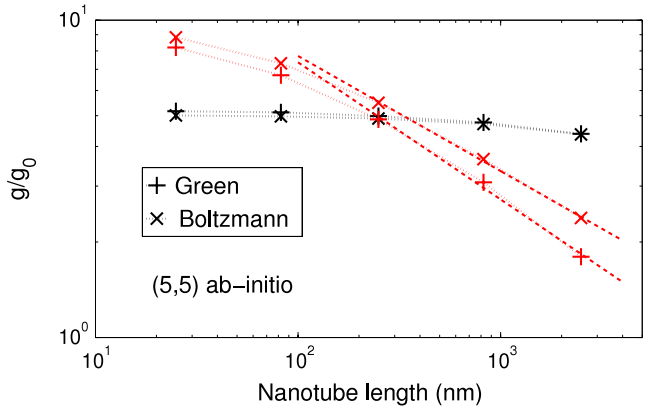

Figure 7. Dotted line: variation of the normalized conductance for temperatures $T = 50$ K (black curves, almost horizontal) and $T = 300$ K (red curves) for the conductivities computed with the Green function and Boltzmann approaches. For a given temperature, the Boltzmann curve is always above the Green's function curve. Dashed lines are estimated scalings of the normalized conductance $\bar{g} \sim L^{-\alpha}$ within the Green function approach: $\alpha = 0.43$ at $T = 300$ K. Recall that, for Fourier's law to hold, the exponent α should be equal to 1.

unit length by assuming that the CNTs used for the experiments have a diameter of 1 nm. The authors of Yu *et al* (2005) indeed find that the CNTs used have a diameter in the range 1–2 nm, occasionally 2–3 nm. If the diameter is indeed 1 nm, then the experimental results are close to the ballistic conductance curve, which means that the thermal transport is nearly ballistic (Yu *et al* 2005). If the diameters are larger, there is a reduction of about 50% of the conductance for the CNTs of experimental lengths (about $L = 2.76$ μm) with respect to the ballistic conductance. This reduction may be attributed to anharmonic effects. We remark that, even in this case, the effect of isotopic disorder should still be noticeable since the results on the conductivities in section 4.4 show that isotope disorder can lead to a reduction of about 80% of the conductance at room temperature for CNTs of experimental lengths.

4.2. Transmission functions for tubes of increasing lengths

We present in this section some transmission functions. These functions are the fundamental tools to study thermal transport since the thermal conductivities or conductances can be obtained from it through (6)–(8). We used the following parameters: $c = 0.5$, and the mass disorder corresponds to replacing ^{12}C by ^{13}C ($\Delta m/m = 1/12$). The qualitative features presented are robust with respect to a smaller disorder concentration, but longer tubes should then be studied. Also, the regularizing parameter $\eta/\omega_{\max}^2 = 10^{-8}$. The transmission is computed for $N_\omega = 200$ points uniformly spaced in the range $0 \leqslant \omega \leqslant \omega_{\max} = 1650$ cm^{-1}. The Boltzmann transmissions are computed in all cases with $N_\omega = 1000$.

Figure 6 compares the transmissions obtained within the Green function approach and the Boltzmann treatment. In all cases, the transmission of disordered systems is lower than the ballistic transmission, obtained for defect-free CNTs, and equal to the number of conducting channels at a given pulsation. The results show that the transmission of acoustic modes is almost unaffected by isotope disorder for the tube lengths considered here. Longer system sizes would be necessary to modify substantially the transmission of these acoustic modes. Higher frequency modes, on the other hand, are damped much faster.

A very precise discussion of the transmission as a function of the system length is done in Savic *et al* (2008), where it is shown that the transmission is mostly of diffusive type, particularly in the central region of the spectrum, where the number of modes is maximal. Localization takes place near band edges and for the highest pulsations.

The Boltzmann transmission is in fair agreement with the Green's function transmission, especially at low frequencies. This is an indication that the transmission is of diffusive type since the transmissions obtained with the Boltzmann approach have a diffusive scaling. At higher frequencies, the Boltzmann transmissions are usually higher than the Green's function ones. This is in analogy with the results for the dimensional chains. This is a consequence of the diffusive behaviour of the Boltzmann transmissions, which decrease slower than the exponentially decreasing transmissions predicted by the Green's function method at higher frequencies.

4.3. Divergence of the thermal conductivity

Having computed the transmission functions, we now analyse the behaviour of the thermal conductance as a function of the system size at different temperatures. Figure 7 presents the normalized thermal conductance as a function of the system length (in log–log scale). Two temperatures are considered: $T = 50$ and 300 K. We have verified that, although the transmission function depends on the realizations of the isotope disorder, they do not change much from one given distribution of random masses to another. Typically, the variations of the thermal conductance are less than 1%.

The scalings obtained for $T = 50$ K show that the transmission regime is quasi-ballistic since the conductance

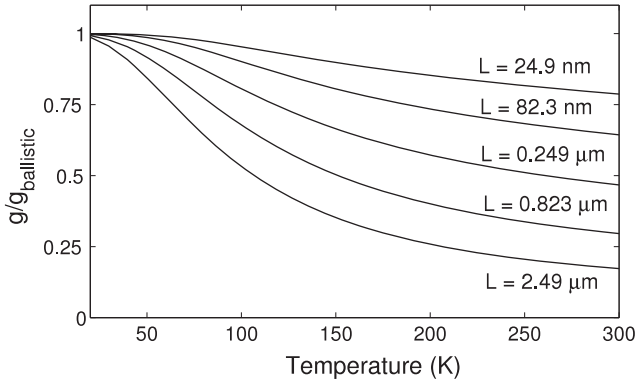

Figure 8. Ratio of the thermal conductance to the ballistic conductance. From top to bottom: increasing tube lengths.

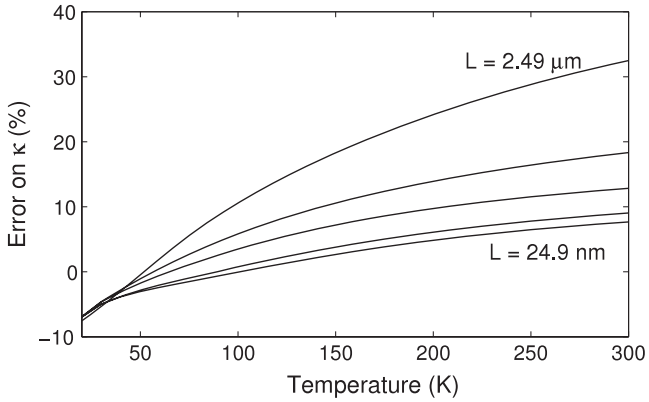

Figure 9. Error on the conductivity computed with the profile obtained from the Boltzmann approach. The reference value is computed from the profiles obtained with the Green's function approach (decreasing lengths from top to bottom; only the first and the last lengths are reported on the curves).

does not change much with the system size. Indeed, at low temperatures, only the low frequencies modes, which are almost unaffected by the disorder, matter. In this regime, the thermal conductivity diverges as the system size.

For higher temperatures ($T = 300$ K), more and more higher frequency modes are introduced, so that disorder has a noticeable effect and the conductance decreases as a function of the system size. The slope α of the different curves has been estimated using some least-squares fitting in order to characterize a power law decay $\bar{g} \sim L^{-\alpha}$, with $\alpha = 0.43$ at $T = 300$ K. The associated thermal conductivities at these temperatures therefore do not converge as the system size is increased:

$$\kappa(L) = gL/\mathcal{A} \sim L^{\beta},$$

with $\beta = 1 - \alpha = 0.57$ for the range of lengths considered in this study. Recall that, for Fourier's law to hold, the thermal conductance should decrease as $\bar{g} \sim L^{-1}$, so that $gL/\mathcal{A}$ converges when L increases.

The asymptotic regime is not yet attained for nanotubes of lengths up to 2.5 μm (which are typical experimental lengths). In this regime the exponent α is not universal since it depends on the tube length and on the amount of mass disorder. As in the case of one-dimensional chains, the truly asymptotic regime corresponds to $\bar{g} \sim L^{-1/2}$ (or $\kappa \sim L^{1/2}$), with associated transmission profiles where only acoustic modes have a non-zero transmission. To this end, much larger system sizes (or a larger mass disorder) should be considered.

In any case, however, it is observed that the conductivity diverges as the system size is increased, since the thermal conductance does not decrease fast enough.

4.4. Reduction of the thermal conductance as a function of the temperature

We study now the temperature dependence of the reduction of the thermal conductance due to isotope defects. Figure 8 presents the thermal conductance of defected CNTs divided by the thermal conductance of defectless CNTs as a function of temperature. Those curves are obtained for the transmission computed with the Green's function approach, but the curves for the transmission computed using a Boltzmann treatment have a very similar behaviour with respect to temperature. Such results were already presented in Savic *et al* (2008) for lower disorder concentrations but with ^{14}C isotope disorder.

As expected, the ratio of the thermal conductance to the ballistic one is always smaller than 1, and converges to 1 in the low temperature limit. Indeed, in the low temperature regime, the thermal transport is due to the acoustic modes only and these modes are almost unaffected by isotope disorder.

Isotopic disorder can be very efficient in reducing the thermal conductivity, especially for tubes of experimental lengths, even at moderately high temperatures. For instance, for tubes of experimental lengths ($L = 2.49$ μm), the thermal conductance is decreased by 80% at room temperature. Notice that the decrease in the thermal conductivity increases with the temperature. This is consistent with the results of the previous sections since, as the temperature is increased, more and more higher frequency modes are introduced and the transmission function is almost a decreasing function of the pulsation.

The thermal conductivity (or conductance) predicted by the Boltzmann approach is compared to the conductivity (or conductance) obtained by the Green's function approach. The results are presented in figure 9, where the error

$$e(T) = \frac{\kappa_{\text{Boltzmann}} - \kappa_{\text{Green}}}{\kappa_{\text{Green}}},$$

is plotted as a function of the temperature T. As can be seen, the Boltzmann approach gives very good estimates of the thermal fluxes in the temperature range considered. It, however, overestimates the conductivity and the error increases with the length of the system and the temperature. This can be explained by the fact that the Boltzmann approach is not precise enough to capture the real decay of the transmission function. In particular, the decrease of the transmission is not fast enough, which is consistent with the results of figure 6.

The good agreement of results obtained with the Boltzmann approach show that Anderson localization, which is not accounted for in the Boltzmann approach, does not have a clear signature in thermal transport for CNTs of experimental

sizes. It also supports the view that thermal transport is CNTs is rather of diffusive type (Savic *et al* 2008).

5. Conclusion

We studied the thermal transport of isotopically disordered harmonic CNTs using Green's function and Boltzmann treatments. In accordance with the theoretical and numerical results for 1D systems (presented in section 3), we expect a divergence of the thermal conductivity with system size in those cases. Our numerical results show that

(i) CNTs described by a harmonic model based on *ab initio* computed force constants share some common features with the thermal transport in isotopically disordered harmonic one-dimensional atom chains, in particular a power law divergence of the thermal conductivity $\kappa(L) \sim L^{\beta}$ (or, equivalently, the thermal conductance does not decrease fast enough, see figure 7). Therefore, no thermal conductivity can be defined and Fourier's law is not valid. For tubes of experimental length, the exponent of the power law divergence $\beta \simeq 0.5$–0.6 at room temperature. For longer tubes, the exponent may well be different since theoretically $\beta = 1/2$ in the asymptotic regime where only the acoustic branches have a non-zero transmission. Experimental results on the length dependence of disordered CNT conductivities, measuring divergences $\beta \simeq 0.4$–0.6 for boron nitride tubes (with a large fraction of mass disorder), have been published in Chang *et al* (2008);

(ii) the thermal conductivity decreases monotonically with the temperature. We showed that there is a dramatic reduction of the thermal conductance for systems of experimental sizes (roughly 80% at room temperature), when a large fraction of isotopic disorder is introduced. This is in accordance with experimental measurements of the effect of isotope disorder in boron nitride nanotubes, which demonstrated dramatic changes in the conductances (a conductance enhancement by 50% for purified materials) (Chang *et al* 2006);

(iii) a Boltzmann description of the thermal transport gives correct results for the thermal conductance even in the presence of Anderson localization. This is particularly interesting since the computation of the transmission using Boltzmann's equation is much less computationally expensive, so that larger systems (such as multi-walled CNTs, boron nitride nanotubes or single-walled CNTs with a large diameter) may be studied with this method. This shows also that Anderson localization, which is not accounted for in the Boltzmann approach, does not have a clear signature in thermal transport for CNTs of experimental sizes. This is also another indication that the transport is of diffusive type (Savic *et al* 2008).

It would now also be interesting to check whether different types of disorder could lead to finite conductivities—in particular, vacancies or functionalized groups. Of course, it would also be possible to combine different types of disorder in order to further reduce the conductivity. As a first-order approximation to the modelling of vacancies, it could be possible to consider defected atoms with very large (infinite) masses, which amounts to neglecting the local geometric rearrangement as compared to actual vacancies. The results would then be very comparable to the results presented here, the precise scalings depending, however, on the concentration of vacancies.

Acknowledgments

We thank Nicola Bonini for the *ab initio* computed interatomic force constants used in this study. Helpful discussions with Nicola Bonini and Nicola Marzari are also acknowledged. Part of this work was done while GS was participating in the programme 'Computational Mathematics' at the Haussdorff Institute for Mathematics in Bonn, Germany.

References

Ashcroft N and Mermin N 1976 *Solid State Physics* (Philadelphia, PA: Saunders)
Baroni S *et al* QUANTUM-ESPRESSO http://www.quantum-espresso.org
Baroni S, de Gironcoli S and Corso A D 2001 *Rev. Mod. Phys.* **73** 515–62
Bonetto F, Lebowitz J and Rey-Bellet L 2000 *Mathematical Physics 2000* ed A Fokas, A Grigoryan, T Kibble and B Zegarlinsky (London: Imperial College Press) pp 128–51
Casher A and Lebowitz J 1971 *J. Math. Phys.* **12** 1701–11
Ceperley D M and Alder B J 1980 *Phys. Rev. Lett.* **45** 566
Chang C, Fennimore A, Afanasiev A, Okawa D, Ikuno I, Garcia H, Li D, Majumdar A and Zettl A 2006 *Phys. Rev. Lett.* **97** 085901
Chang C W, Okawa D, Garcia H, Majumdar A and Zettl A 2008 *Phys. Rev. Lett.* **101** 075903
Datta S 2000 *Superlatt. Microstruct.* **28** 253–78
Datta S 2005 *Quantum Transport: From Atom to Transistor* (Cambridge: Cambridge University Press)
Dhar A 2001 *Phys. Rev. Lett.* **86** 5882–5
Dhar A and Roy D 2006 *J. Stat. Phys.* **125** 805–24
Economou E 2006 *Green's Function Methods in Quantum Physics* 3rd edn (Berlin: Springer)
Fuchs M and Scheffler M 1999 *Comput. Phys. Commun.* **119** 67
Furstenberg H 1963 *Trans. Am. Math. Soc.* **108** 377–428
Hone J, Whitney M, Piskoti C and Zettl A 1999 *Phys. Rev.* B **59** R2514–6
Ishii K 1973 *Suppl. Prog. Theor. Phys.* **45** 77–138
Jaksic V 2006 *Topics in Spectral Theory* (*Lecture Notes in Mathematics* vol 1880) (Berlin: Springer) pp 235–312
Keller J, Papanicolaou G and Weilenmann J 1978 *Commun. Pure Appl. Math.* **32** 583–92
Lepri S, Livi R and Politi A 2003 *Phys. Rep.* **377** 1–80
Lukkarinen J and Spohn H 2007 *Arch. Ration. Mech. Anal.* **183** 93–162
Matsuda H and Ishii K 1970 *Suppl. Prog. Theor. Phys.* **45** 56–86
Mingo N and Broido D 2005a *Phys. Rev. Lett.* **95** 096105
Mingo N and Broido D 2005b *Nano Lett.* **5** 1221–5
Mounet N 2005 *Master Thesis*
O'Connor A and Lebowitz J 1974 *J. Math. Phys.* **15** 692–703
Pop E, Mann D, Wang Q, Goodson K and Dai H 2006 *Nano Lett.* **6** 96–100
Rego L and Kirczenow G 1998 *Phys. Rev. Lett.* **81** 232–5
Rieder Z, Lebowitz J and Lieb E 1967 *J. Math. Phys.* **8** 1073–8
Rubin R 1968 *J. Math. Phys.* **9** 2252–66
Rubin R and Greer W 1971 *J. Math. Phys.* **12** 1686–701
Savic I, Mingo N and Stewart D A 2008 *Phys. Rev. Lett.* **101** 165502

Schwab K, Henriksen E, Worlock J and Roukes M 2000 *Nature* **404** 974–7
Simon F, Kramberger C, Pfeiffer R, Kuzmany H, Zolyomi V, Kurti J, Singer P and Alloul H 2005 *Phys. Rev. Lett.* **95** 017401
Spohn H 2006 *J. Stat. Phys.* **124** 1041–104
Stoltz G, Lazzeri M and Mauri F 2008 arXiv:0810.1830
Tamura S 1983 *Phys. Rev.* B **27** 858–66
Troullier N and Martins J L 1991 *Phys. Rev.* B **43** 1993
Vandecasteele N, Lazzeri M and Mauri F 2009 *Phys. Rev. Lett.* **102** 196801
Wang Z, Tang D, Zheng X, Zhang W and Zhu Y 2007 *Nanotechnology* **18** 475714
Widulle F, Serrano J and Cardona M 2002 *Phys. Rev.* B **65** 075206
Yamamoto T, Nakazawa Y and Watanabe K 2007 *New J. Phys.* **9** 245
Yu C, Shi L, Yao Z, Li D and Majumdar A 2005 *Nano Lett.* **5** 1842–6
Zhang W, Fisher T and Mingo N 2007 *Numer. Heat Transfer* B **51** 333–49